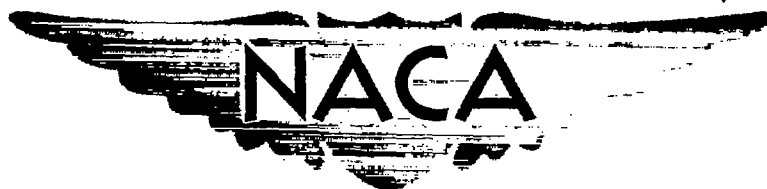


NACA RM E54D28

4889



Req # 17074

JAN 31 1957

DL43288



TECH LIBRARY KAFB, NM

RESEARCH MEMORANDUM

INITIAL PERFORMANCE INVESTIGATION OF PENTABORANE FUEL
IN FREE-FLIGHT RAM-JET ENGINE

By John H. Disher and Leonard Rabb

Lewis Flight Propulsion Laboratory
Cleveland, Ohio

Classification cancelled (or changed to ~~UNCLASSIFIED~~)
By Authority of *NASA Tech Rep. Aeronaut. 15*
(OFFICER AUTHORIZED TO CHANGE)

By *2 Apr 57*
NAME AND

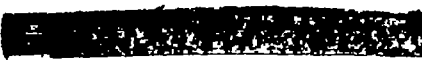
HRB
GRADE OF OFFICER MAKING CHANGE)

3 Apr 61
DATE


NATIONAL ADVISORY COMMITTEE
FOR AERONAUTICS

WASHINGTON
January 24, 1957

~~CONFIDENTIAL~~





NATIONAL ADVISORY COMMITTEE FOR AERONAUTICS

RESEARCH MEMORANDUMINITIAL PERFORMANCE INVESTIGATION OF PENTABORANE FUEL IN
FREE-FLIGHT RAM-JET ENGINE

By John H. Disher and Leonard Rabb

SUMMARY

In order to evaluate one of the more promising high-energy fuels under actual flight conditions, a 9.75-inch-diameter ram jet utilizing pentaborane fuel has been flown. The engine was released from a carrier airplane at 31,000 feet and a Mach number of 0.56. During descent, the engine accelerated to a Mach number of 1.45 when a flame-out believed due to spray-bar failure took place.

During the flight, most of which took place under severe combustor inlet conditions, an average combustion efficiency of 94 percent was observed. This efficiency compares with the 70 percent obtained with JP-3 fuel under similar conditions. Because of these differences in combustion efficiency, as well as the high heating value of pentaborane, the range of a missile with pentaborane fuel under the average conditions of this flight was calculated to be 70 percent greater than with JP-3 under the same conditions.

High diffuser total-pressure losses were observed between Mach numbers of 1.13 and 1.4 due to shock interaction effects which accompanied the high heat release and low mass-flow ratios sustained during the flight.

A maximum thrust coefficient of 0.645 was observed at a Mach number of 1.10 and a maximum thrust-minus-drag coefficient of 0.31 was observed at a Mach number of 0.93. These values occurred with a total-temperature-ratio parameter of approximately 7.0.

INTRODUCTION

Theoretical analyses have indicated the significant performance gains to be realized by the use of high-energy fuels in ram-jet and turbojet engines. Laboratory tests have confirmed many of these theoretical advantages. In July, 1953 the Navy Bureau of Aeronautics felt that these

laboratory tests had reached a point where an actual flight evaluation of one of the most promising high-energy fuels was in order, and the NACA was requested to conduct such an investigation with pentaborane fuel. The vehicle selected for these flight tests was a 9.75-inch-diameter ram-jet engine similar to the gasoline-fueled 16-inch-diameter engine previously flown by the NACA. The combustor configuration for the engine was derived by connected-pipe tests, which are being reported separately. The flight tests are carried out by launching the fin stabilized unguided engines from a carrier plane (fig. 1) at high altitude. Data are obtained during descent by means of radar and telemetering.

Reported herein are results from the initial flight investigation of pentaborane fuel.

SYMBOLS

The following symbols are used in this report:

A	cross-sectional area
A_{lip}	projected area of the cowl lip, 0.251 sq ft
A_0	free-stream tube area, sq ft
a_η	acceleration exclusive of gravity, gravitational units
C_D	drag coefficient, $D/q_0 A_{max}$
C_F	thrust coefficient, $F/q_0 A_{max}$
$(C_F - C_D)$	net propulsive force coefficient, $a_\eta W_e / q_0 A_{max}$
D	drag, lb
F	thrust, lb
f/a	fuel-air ratio
g	acceleration due to gravity, 32.17 ft/sec ²
l	body length (118.4 in.), 9.87 ft
M	Mach number
m/m_0	mass-flow ratio, A_0/A_{lip}

P	total pressure, lb/sq ft
p	static pressure, lb/sq ft
q_0	free-stream dynamic pressure, $0.7 p_0 M_0^2$, lb/sq ft
R	gas constant
Re	Reynolds number, $V_0 l \rho_0 / \mu_0$
S_a	air specific impulse, (lb)(sec)/lb air
T	total temperature, °R
t	static temperature, °R
V	velocity, ft/sec
W_e	weight of the engine at a given time
W_f	fuel flow, lb/hr or lb/sec
η_b	combustion efficiency, $(\Phi_{\text{theoretical}} / \Phi_{\text{exp}}) S_a$ constant
θ	time, sec
μ	ratio of gas flow to air flow, ω_g / ω_a
μ	absolute viscosity, (lb)(sec)/sq ft
$\mu^2 \frac{R_6}{R_5} \tau$	heat-addition parameter
ρ	density, slugs/ft ³
τ	total-temperature ratio across the combustion chamber
Φ	equivalence ratio, (f/a)/stoichiometric mixture
ω_a	air flow through the engine, lb/sec
ω_g	gas flow at exit, lb/sec

Subscripts:

0	free-stream conditions
1	inlet station
2	air-flow station
3	diffuser exit station
4	fictitious station which has the same total pressure and air flow as at station 3 and with area equal to that at station 5
5	station immediately behind the flame holder
6	exit station
exp	experimental
max	maximum
th	theoretical

APPARATUS AND INSTRUMENTATION

The ram-jet engine investigated was designed with a 25° half-angle conical nose inlet which was similar to that described in reference 1. The cone was positioned axially to permit the oblique shock to intercept the cowl lip at the design Mach number of 1.8. A long slender probe protruded from the apex of the cone and was used to obtain the free-stream static and total pressures in addition to acting as a radio-telemetering antenna. The geometry of the centerbody or "island" was such that the diffuser had no internal contraction.

The radio-telemetering equipment was located in the forward part of the centerbody as shown in figure 2 and the remaining volume was allotted to the fuel system. The fuel system has been adequately described in reference 2 and only minor changes have been made in keeping with the safety requirements for pentaborane. The fuel was retained in the piston type tank until release by an aluminum-foil burst disk as shown in figure 2. Teflon was used in place of rubber for "O" ring seals in the system. A regulated flow of helium gas controlled the movement of the piston to give the desired fuel flow.

The spray-bar and flame-holder configuration shown in figure 3 were developed by connected-pipe tests which will be reported separately.

The spray bar gives approximately a linear flow pressure characteristic through use of a spring-loaded piston in the center. The eight radial spokes of the spray bar fit between the flame-holder elements, and fuel discharges from 3 upstream facing holes in each spoke. A magnesium flare with 20-second burning time is mounted in the center of the flame holder for ignition.

The ram jet weighed 156 pounds fully loaded which included 8.77 pounds of fuel; the center of gravity of the engine was located at station 56.35.

The instrumentation consisted of an eight-channel radio-telemetering unit which transmitted the following information to two ground receiving stations:

1. Free-stream static pressure
2. Free-stream total pressure
3. Static pressure at air-flow station 2 (22 in. downstream of inlet)
4. Total minus static pressure at station 2
5. Free-stream total minus diffuser exit total pressure at station 3 (65 in. downstream of inlet)
6. Exit static pressure at station 118.4
7. Regulated fuel system helium pressure minus diffuser exit total pressure
8. Net acceleration (axial)

Continuous colored motion pictures of the flight were obtained with cameras in the launching airplane and at the ground station.

CALCULATION PROCEDURE

An atmospheric survey was made by the carrier airplane immediately after the ram-jet test engine was launched. The variation of ambient pressure and temperature with true altitude was obtained by radar-tracking the descending aircraft. The free-stream velocity of the ram-jet relative to the ambient air was determined from the ratio of the free-stream static and total pressures as obtained from the instrumentation on the ram-jet antenna. The free-stream velocity was also obtained from the radar data by differentiating the space position against time

curve and also by integrating the accelerometer and correcting the results of both methods for any winds aloft. The wind corrections were obtained by radar tracking a weather balloon, which was released from the ground station immediately following the survey. The free-stream Mach number, total temperature, and total pressure were calculated as in reference 3. The air flow through the engine was obtained from the instrumentation at station 2 and the flow conditions at station 4 were computed on the basis of the mass continuity equation. An assumed loss in the total pressure across the flame holder ($P_5 - P_4$) of $2q_4$ was used to obtain the Mach number at station 5 from that calculated for station 4.

The thrust coefficient C_F and combustion efficiency η_b are defined by equations (1) and (2):

$$C_F = \left[\frac{(\dot{w}_a + \dot{w}_f)V_6}{g} + (P_6 - P_0)A_6 - \frac{\dot{w}_a}{g} V_0 \right] / 0.7 P_0 M_{O_{\max}}^2 \quad (1)$$

$$\eta_b = \left(\frac{\Phi_{th}}{\Phi_{exp}} \right)_{S_a \text{ constant}} \quad (\text{ref. 4}) \quad (2)$$

The theoretical equivalence ratio Φ_{th} is a function of the gas total temperature T_6 and inlet total temperature T_0 . The gas total temperature T_6 was obtained in the manner of reference 3 with due consideration for the nongaseous oxides in the products of combustion (ref. 4).

A combustion pressure of 2 atmospheres was assumed in considering the effects of the nongaseous oxides in the products of combustion. Reference 4 indicates the pressure level is of some importance at equivalence ratios near 0.4, but does not indicate the magnitude of the error.

The drag coefficient was obtained from equation (3)

$$C_D = C_F - (C_F - C_D) \quad (3)$$

where

$$C_F - C_D = \frac{W_{\text{engine}} \eta}{q_0 A_{\max}} \quad (4)$$

Fuel flow was calculated from the differential pressure across the fuel nozzle and a preflight calibration of the fuel spray bar. For safety, helium pressure was measured rather than fuel pressure and the

slight pressure drop across the fuel tank piston and in the fuel system, as obtained during preflight tests, was subtracted from the measured pressure differential.

RESULTS AND DISCUSSION

Time History

The time history of the missile flight is presented in figures 4 and 5. Figure 4 presents the altitude, Mach number, acceleration (exclusive of gravity), Reynolds number, velocity, and free-stream pressures and temperatures encountered during the flight. The model was launched from the carrier plane at a pressure altitude of 31,170 feet and a Mach number of 0.56. The model accelerated to a Mach number of about 1.45 at 31 seconds after release when a flame-out occurred for about 1 second, followed by a 6/10-second burst of burning and a second flame-out. At 31 seconds, the model was at a pressure altitude of 13,000 feet and was accelerating at the rate of approximately 2 g's. During the 6/10-second burst of burning, the acceleration varied from 5.8 to 2.5 g's. After the second flame-out the model decelerated until impact occurred 42.7 seconds after release. Colored motion pictures showed the model burning with an intense whitish-green flame extending several feet behind the engine throughout the burning portion of the flight.

Figure 5 presents the time history of the combustion performance. The combustor inlet static temperature and pressure and velocity are shown in figure 5(a). Figure 5(b) presents the time history of fuel flow, fuel-air ratio, gas total-temperature ratio across the combustion chamber τ , and the combustion efficiency.

During the first 20 seconds of the flight, the combustor inlet pressure varied from about $1/3$ to $2/3$ atmosphere and these pressures were accompanied by combustor inlet temperatures of 425° to 480° R. Under these severe conditions, combustion efficiencies of the order of 90 to 100 percent were observed. Under comparable conditions, with gasoline, maximum efficiencies of the order of 70 percent were observed in flight (ref. 5) and 85 to 90 percent in connected-pipe tests (refs. 6 and 7). A comparison of the combustor efficiencies observed in flight with those observed during connected-pipe tests with pentaborane is shown in figure 6. The efficiencies were of the same order.

In discussing possible reasons for the flame-out at 31 seconds, it will be helpful to refer to excerpts from actual telemeter records which are reproduced in figure 7. The short record excerpt from 22.5 to 23.0 seconds is typical of the smooth burning during the flight up to about 27.5 seconds after release. No indication of pulsating flow

is apparent. At about 27.5 seconds ($M_0 \approx 1.2$) slight pulsations in air flow and acceleration begin; these pulsations increased in amplitude as the vehicle accelerated and reached a maximum at about 30.6 seconds. At about 30.6 seconds the heat addition in the combustor chamber fell off as indicated by a rise in air flow; the heat addition continues to drop until, at about 31.1 seconds, combustion ceased, and acceleration fell to about -4 g's. At 32.08 seconds reignition occurred and burning continues to about 32.7 seconds when flame-out again occurred.

It is significant that no change in helium pressure (which actuates the fuel tank piston) preceded the first indication of falling heat release at 30.5 seconds. Two possible explanations for the drop in heat release and subsequent flame-out are: (a) the spray bar may have plugged and prevented further fuel flow, or (b) the fuel may have been released at a high rate because of burning away of the fuel spray bar. It is possible that the resulting high rate of fuel flow quenched the burning and that the reignition at 32.08 seconds occurred as the last of the fuel was discharged and the mixture came into a combustible range as the fuel flow went to zero. The behavior of the helium pressure measurement between 31 and 32 seconds tends to confirm the second explanation.

At 31.1 seconds, as the engine went out, the helium pressure started to decrease at a rate appreciably greater than could be accommodated by the regulator bleed if the fuel-flow rate corresponded to the nozzle calibration. At 32.03 seconds, shortly before reignition, the helium pressure started to rise, although the control pressure does not call for an increase until reignition at 32.08 seconds. It is believed that the rapid drop in helium pressure was due to fuel discharge at a high rate following spray-bar failure, and that the subsequent rise in helium pressure just before reignition indicates that the fuel tank piston approached bottom at that point. It was calculated that 2.93 pounds (33 percent) of fuel remained in the tank at 30.5 seconds, when the first indication of falling heat release occurred. If this quantity of fuel were discharged between 30.5 and 32.0 seconds, the fuel-air ratio would be several times the stoichiometric value.

If the "fuel dumping" explanation is correct, it is probable that the pulsating flow contributed to the spray-bar failure through upstream burning.

The pulsating flow is believed to have been caused by inlet instability resulting from the low mass-flow ratios which accompany the high combustion-chamber heat addition. If the pulsations were caused by rough combustion, they should have occurred at subsonic as well as supersonic speeds. The mass-flow ratios for the engine are plotted against Mach number in figure 8; for comparison, the maximum possible or "critical" mass-flow ratio for the inlet is also shown.

Pressure Recovery

333 9

The total-pressure recovery at the subsonic diffuser exit P_3/P_0 and at station 2 P_2/P_0 are presented in figure 9 against the free-stream Mach number with indicated mass-flow ratios m/m_0 as a parameter. The subsonic diffuser loss between stations 2 and 3 was 3 to 6 percent throughout the burning portion of the flight. The decrease in the over-all diffuser pressure recovery P_3/P_0 at Mach numbers greater than 1.13 was attributed to shock-boundary-layer interaction effects which accompanied the high heat release and low mass-flow ratios. At a Mach number of 1.38 and m/m_0 of about 0.65, P_3/P_0 was 0.846 and P_2/P_0 was 0.897, indicating that about 2/3 of the total-pressure loss took place at the inlet and in the first 22 inches of subsonic diffuser, with the other 5 percent occurring in the remaining 43 inches of subsonic diffuser. The ram jet experienced a 23-cycle-per-second buzz beginning at Mach number 1.23 during the burning portion of the flight. The data points therefore represent average total-pressure recoveries and not instantaneous values for Mach numbers greater than 1.23. Figure 9 also presents P_3/P_0 against free-stream Mach number when the ram jet was not burning. The shock was inside the diffuser and P_3/P_0 was 0.613 at Mach number 1.415. A cross-plot of the data of figure 9 is shown in figure 10 at a free-stream Mach number of approximately 1.4. The subsonic diffuser loss between stations 2 and 3 diminished slightly as m/m_0 decreased, but the over-all recovery dropped markedly, indicating that most of the loss was occurring near the inlet. The total-pressure loss at station 2 was only 1 percent at m/m_0 of 0.90, but increased to 10.5 percent at m/m_0 of 0.65. The 16-inch-diameter engines described in reference 5 did not show comparable losses and the pressure recovery was observed to increase with decreasing m/m_0 at 1.4 Mach number. Differences in subsonic diffuser design or the relatively larger antenna probe on the 9.75-inch-diameter engine may explain the different pressure-recovery characteristics of the 9.75- and the 16-inch-diameter engines.

Thrust, Thrust-Minus-Drag, and Drag Coefficient

The thrust coefficient of the ram jet is presented in figure 11 against the free-stream Mach number. Also shown are values of the heat-addition parameter $\mu^2 \frac{R_6}{R_5} \tau$. The loss in total-pressure recovery previously discussed is reflected in the drop in thrust coefficient following Mach number of approximately 1.10. The maximum thrust coefficient was 0.645 at a Mach number of approximately 1.10. The internal drag of the ram jet observed during missile deceleration with no heat addition is also shown in figure 11.

The thrust-minus-drag coefficient and the drag coefficient are presented in figures 12 and 13, respectively, with indicated mass-flow ratios. The thrust-minus-drag coefficient $C_F - C_D$ increased from 0.167 at a Mach number of 0.670 to 0.31 at Mach number of 0.932 for approximately constant mass-flow ratio of 0.55. A minimum $C_F - C_D$ of 0.135 occurred at Mach number of 1.12. The decrease in $C_F - C_D$ between Mach numbers of 0.932 and 1.12 may be partially explained as due to the transonic drag rise. However, the sudden increase in $C_F - C_D$ at Mach number of 1.15 occurred when the thrust coefficient was decreasing and could only mean a rapid decrease in the drag coefficient (fig. 13). The exact nature of this sudden decrease in the drag coefficient which occurred at a relatively constant mass-flow ratio is not understood. The external drag coefficient of the ram jet after flame-out is also given in figure 13 and represents the minimum external drag possible for the engine. The increase in drag for the burning engine represents the additive drag penalty incurred when the engine operates at low mass-flow ratios. It is apparent from the appreciable drag rise above the minimum values that at these low mass-flow ratios, cowl suction has not offset additive drag to any great extent.

Comparison with Hydrocarbon Fuel

A graph comparing pentaborane with JP-3 in terms of relative range is shown in figure 14. These comparisons are based on the actual performance of the engine during this flight and on the calculated performance of the same engine under the same conditions with the same weight of JP-3. Relative range is defined as the ratio of the range of a missile with the stated fuel and efficiency to the range of a similar missile with JP-3 fuel and 100 percent combustion efficiency. Except for effects of fuel density, which are slight for the two fuels considered here, relative range is directly proportional to fuel weight specific impulse as shown in reference 8. The values shown in figure 14 are an average for the flight conditions between 10 and 30 seconds after release during which the average pentaborane equivalence ratio was approximately 0.55. The ideal pentaborane and JP-3 performance under the flight conditions were calculated from the data of reference 4 and the actual JP-3 performance was based on the combustion efficiency obtained with JP-3 fuel in the 16-inch-diameter engines of reference 5.

For the average of the flight conditions, the relative range with pentaborane and 100 percent combustor efficiency would be 1.28. At appreciably lower equivalence ratios than utilized in this flight, the theoretical relative range for pentaborane is approximately 1.5 as shown in reference 8. With the actual observed combustion efficiency of this flight, the relative range was 1.2, or about 6 percent less than idealized for the average conditions. In other words, 94 percent of the theoretical effective heat content of the pentaborane was realized in this flight.

3339 Based on actual performance in the 16-inch-diameter engines, the relative range for JP-3 is reduced to 0.70. Thus, under similar conditions, pentaborane shows about 70 percent greater range than JP-3. It is known that with sufficient development, combustion efficiencies of the order of 85 to 90 percent could be obtained with JP-3 under the average flight conditions. If a comparison is made on this basis, pentaborane will show about a 40 percent improvement in relative range. Although these relative values were obtained at comparatively low Mach numbers, the comparisons are applicable to high Mach numbers at high altitudes where combustor inlet conditions are of a severity comparable to those encountered in this flight.

One factor which may affect the performance of pentaborane and which has not as yet been investigated, is the performance of this fuel in a high expansion ratio nozzle where high exit Mach numbers will be encountered. In this case, failure of oxides in the exhaust to maintain velocity equilibrium with the gaseous exhaust products could lead to significant thrust losses as compared with hydrocarbon fuels under similar conditions.

SUMMARY OF RESULTS

The initial flight test of pentaborane fuel in a 9.75-inch-diameter air-launched ram jet has provided the following results:

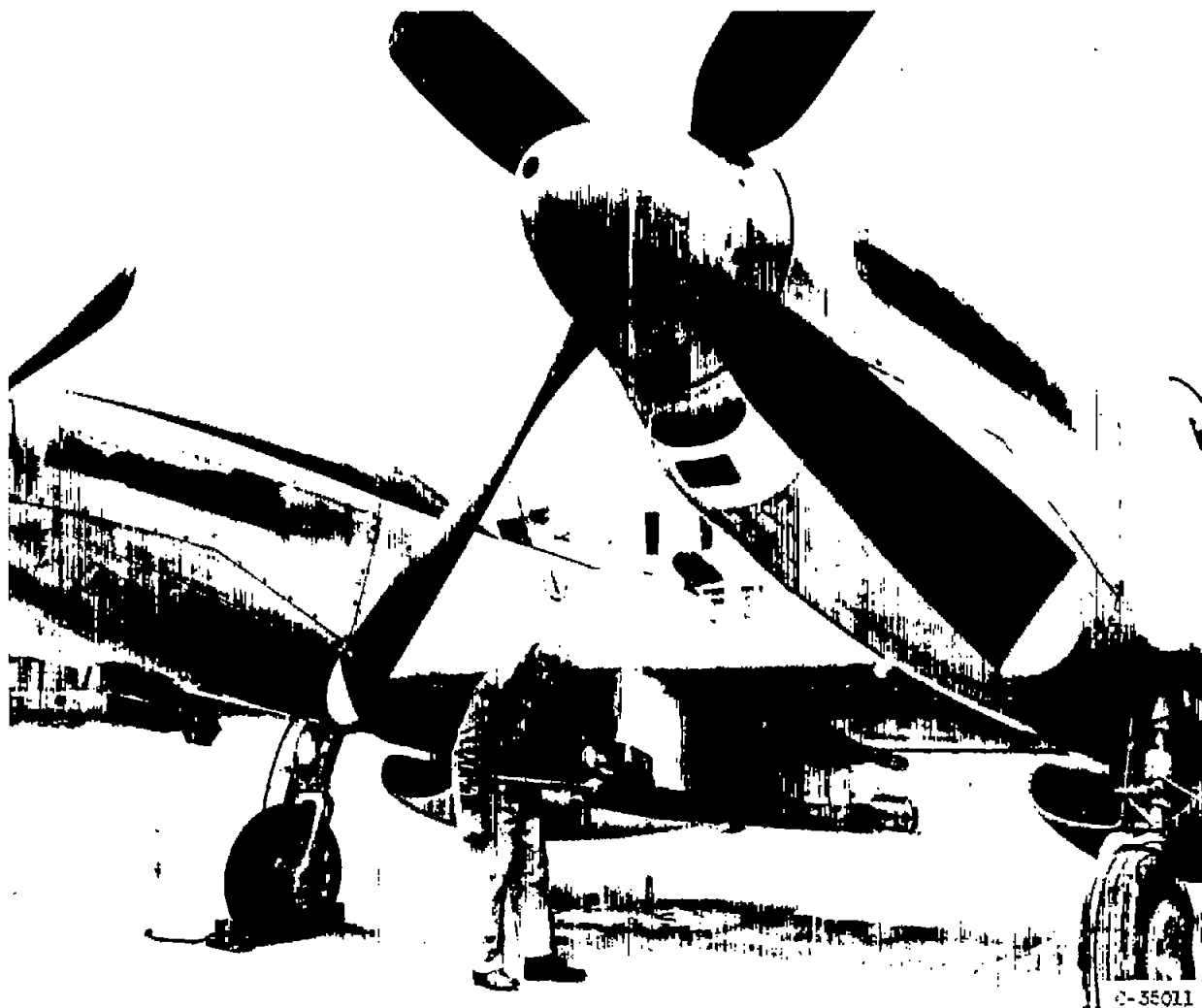
1. The engine accelerated from the launching Mach number of 0.56 to a Mach number of about 1.45, 31 seconds after release when a flame-out believed due to fuel spray-bar failure occurred.
2. An average combustion efficiency of 94 percent was observed during the flight. This compares with about 70 percent obtained in flight with JP-3 in 16-inch-diameter engines under similar conditions.
3. For the average of the flight conditions, pentaborane fuel was calculated to give 70 percent greater range than would be obtained with JP-3 under the same conditions. This advantage reduces to 40 percent if it is assumed that by further development an average combustion efficiency of 85 percent could be realized in flight with JP-3 under these conditions.
4. High diffuser total-pressure losses were observed between Mach numbers of 1.13 and 1.40 due to shock interaction effects which accompanied the high heat release and low mass-flow ratios sustained during the flight.
5. A maximum thrust coefficient of 0.645 was observed at a Mach number of 1.10 and a maximum thrust-minus-drag coefficient of 0.31 was

observed at a Mach number of 0.93. These values occurred with a total temperature ratio parameter of approximately 7.0.

Lewis Flight Propulsion Laboratory
National Advisory Committee for Aeronautics
Cleveland, Ohio, April 27, 1954

REFERENCES

1. Disher, John H., and Rabinowitz, Leonard: Free-Flight Performance of 16-Inch-Diameter Supersonic Ram-Jet Units. III - Four Units Designed for Combustion-Chamber-Inlet Mach Numbers of 0.245 at Free-Stream Mach Number of 1.8 (Units D-1, D-2, D-3, and D-4). NACA RM E50D07, 1950.
2. Disher, John H., Kohl, Robert C., and Jones, Merle L.: Free-Flight Performance of a Rocket-Boosted Air-Launched 16-Inch-Diameter Ram-Jet Engine at Mach Numbers up to 2.20. NACA RM E52L02, 1953.
3. Carlton, William W., and Messing, Wesley E.: Free-Flight Performance of 16-Inch-Diameter Supersonic Ram-Jet Units. I - Four Units Designed for Combustion-Chamber-Inlet Mach Number of 0.12 at Free-Stream Mach Number of 1.6 (Units A-2, A-3, A-4, and A-5). NACA RM E9F22, 1949.
4. Tower, Leonard K., and Gammon, Benson E.: Analytical Evaluation of Effect of Equivalence Ratio, Inlet-Air Temperature, and Combustion Pressure on Performance of Several Possible Ram-Jet Fuels. NACA RM E53G14, 1953.
5. North, Warren J.: Summary of Free-Flight Performance of a Series of Ram-Jet Engines at Mach Numbers from 0.80 to 2.20. NACA RM E53K17, 1954.
6. Henzel, James G., Jr., and Wentworth, Carl B.: Free-Jet Investigation of 20-Inch Ram-Jet Combustor Utilizing High-Heat-Release Pilot Burner. NACA RM E53H14, 1953.
7. Rayle, Warren D., and Koch, Richard G.: Design of Combustor for Long-Range Ram-Jet Engine and Performance of Rectangular Analog. NACA RM E53K13, 1954.
8. Henneberry, Hugh M.: Effect of Fuel Density and Heating Value on Ram-Jet Airplane Range. NACA RM E51L21, 1952.



C-35011

Figure 1. - 9.75-Inch ram jet mounted on carrier airplane.

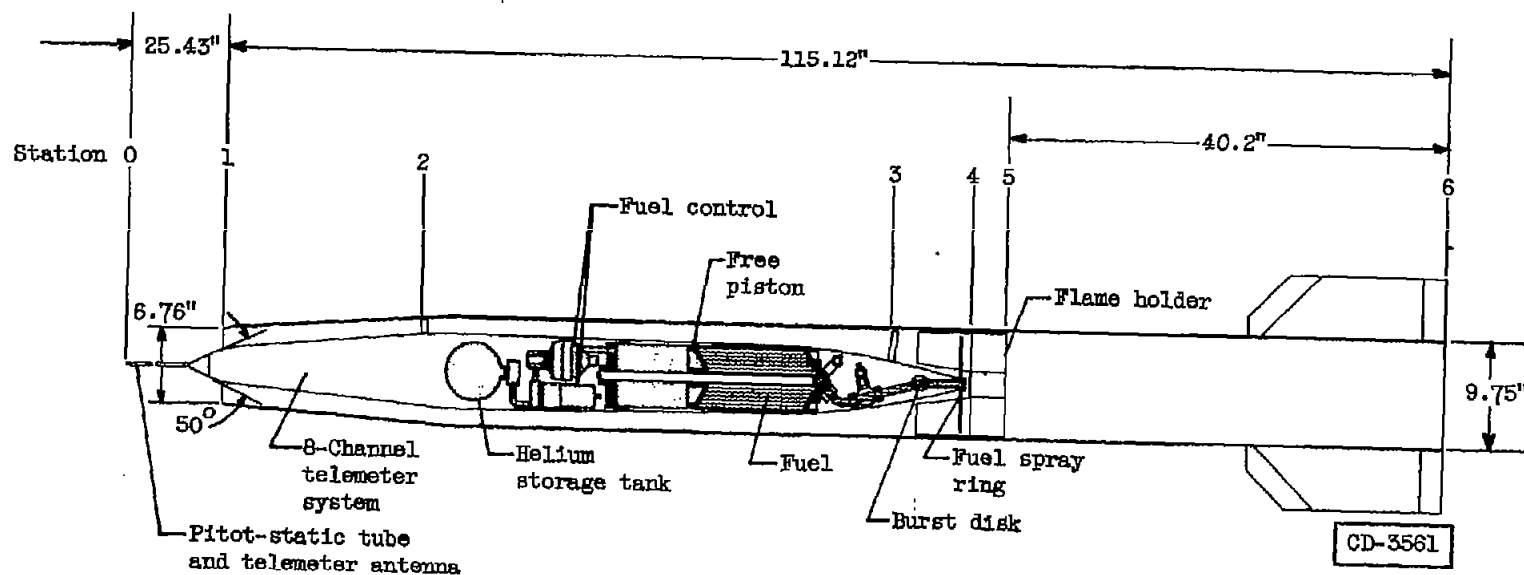
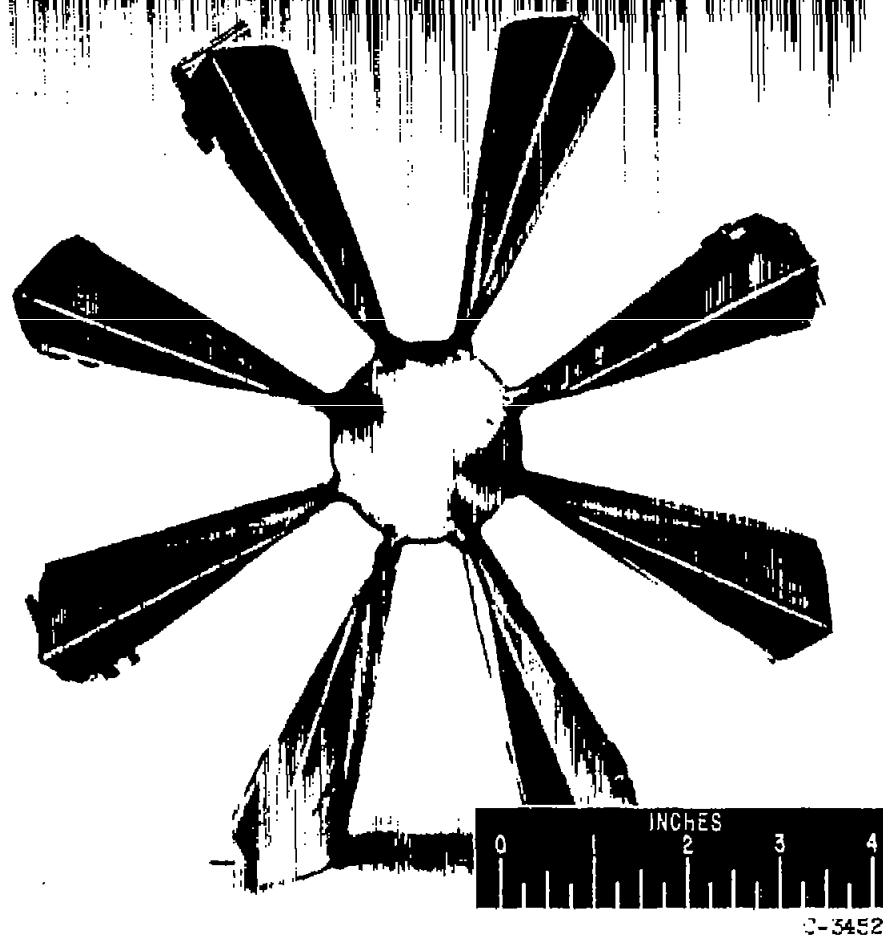


Figure 2. - Sketch of 9.75-inch-diameter free-flight ram jet for high-energy-fuel tests.



(a) Flame holder.

Figure 3. - Flame holder and fuel spray bar for 9.75-inch ram jet.

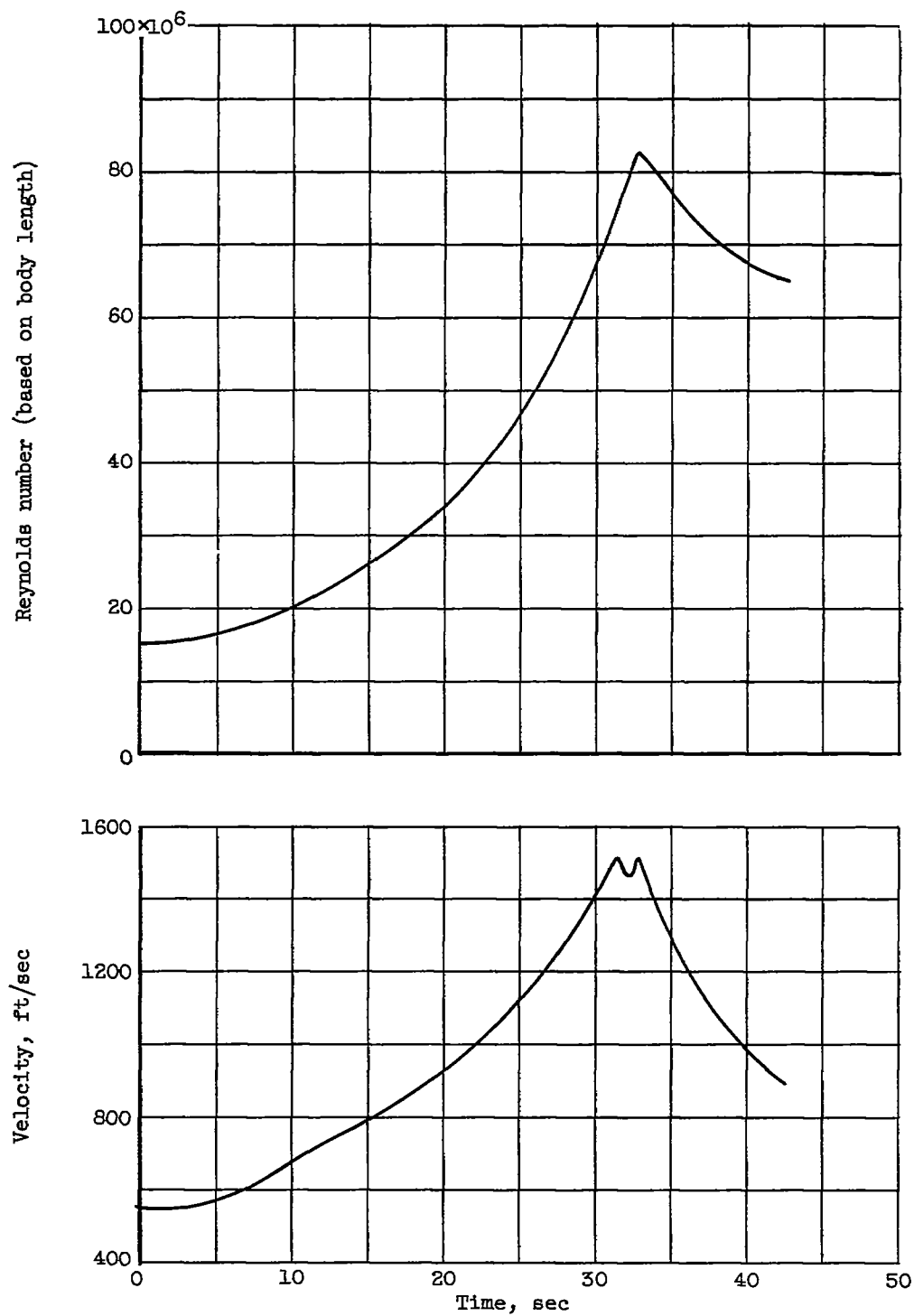
CONFIDENTIAL

NACA RM E54D28

C-34812

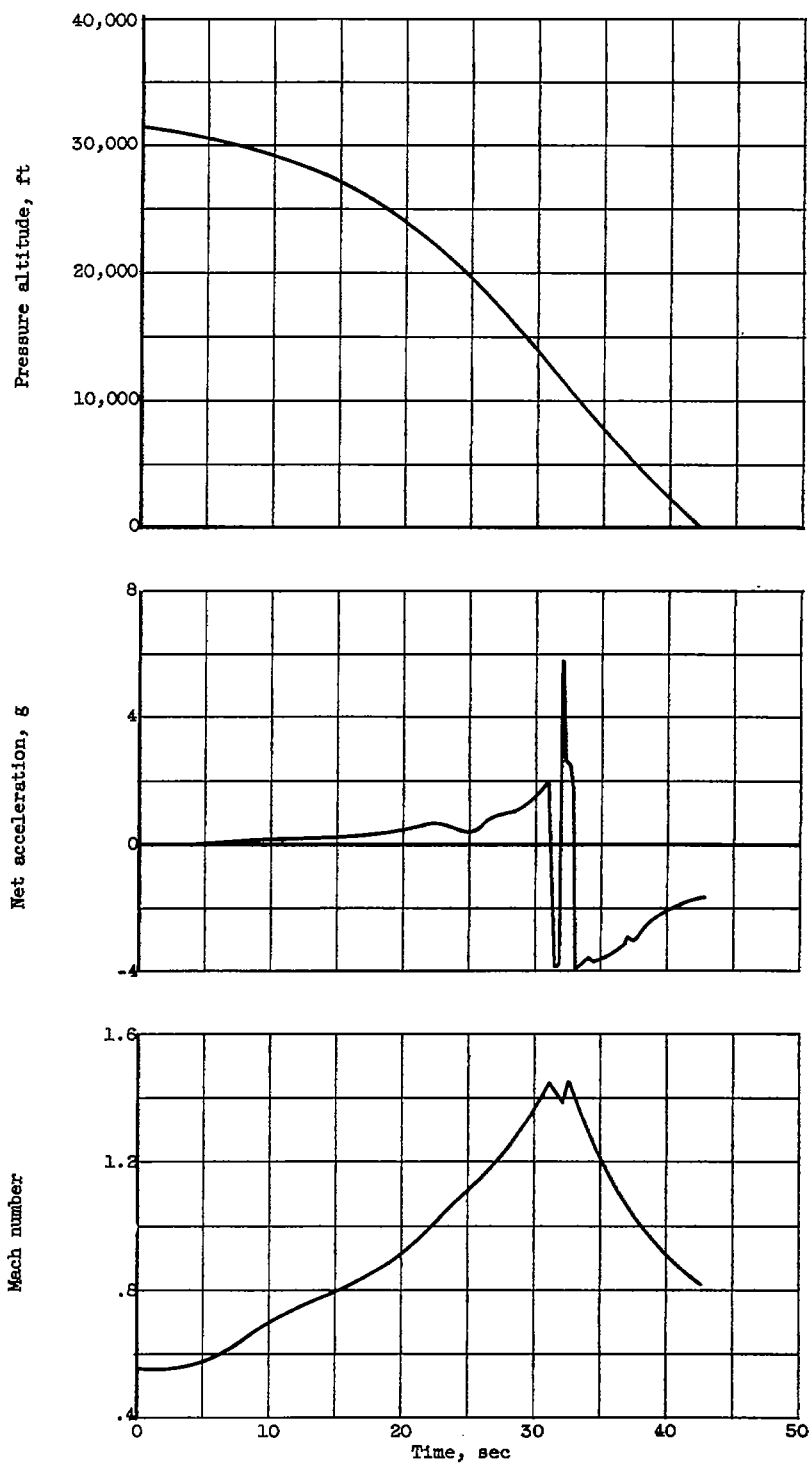
(b) Fuel spray bar in fuel discharge end of ram-jet center body.
Figure 3. - Concluded. Flame holder and fuel spray bar for 9.75-inch ram jet.

3339



(a) Reynolds number and velocity.

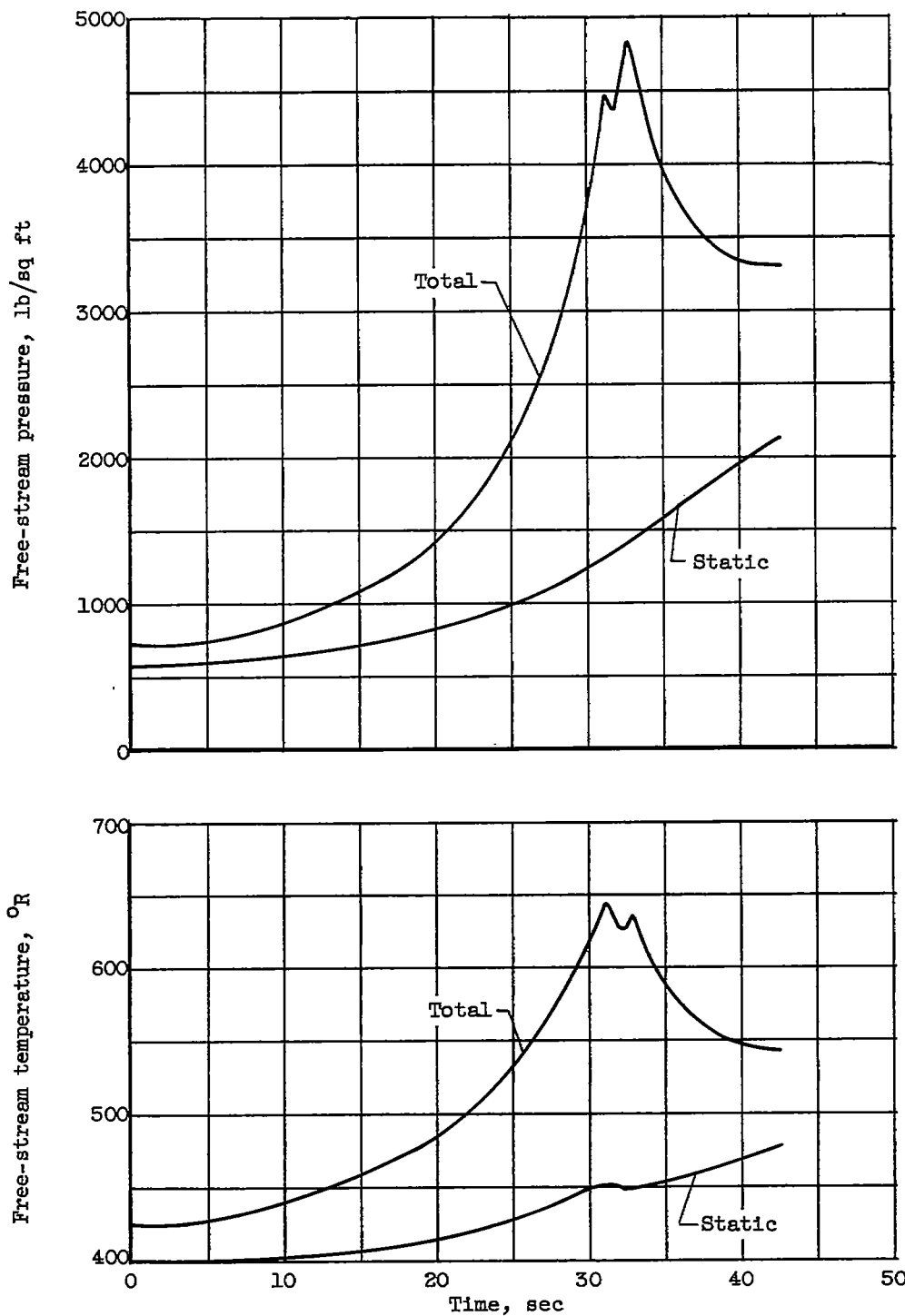
Figure 4. - Time history of flight conditions.

~~CONFIDENTIAL~~

(b) Mach number, acceleration, and pressure altitude.

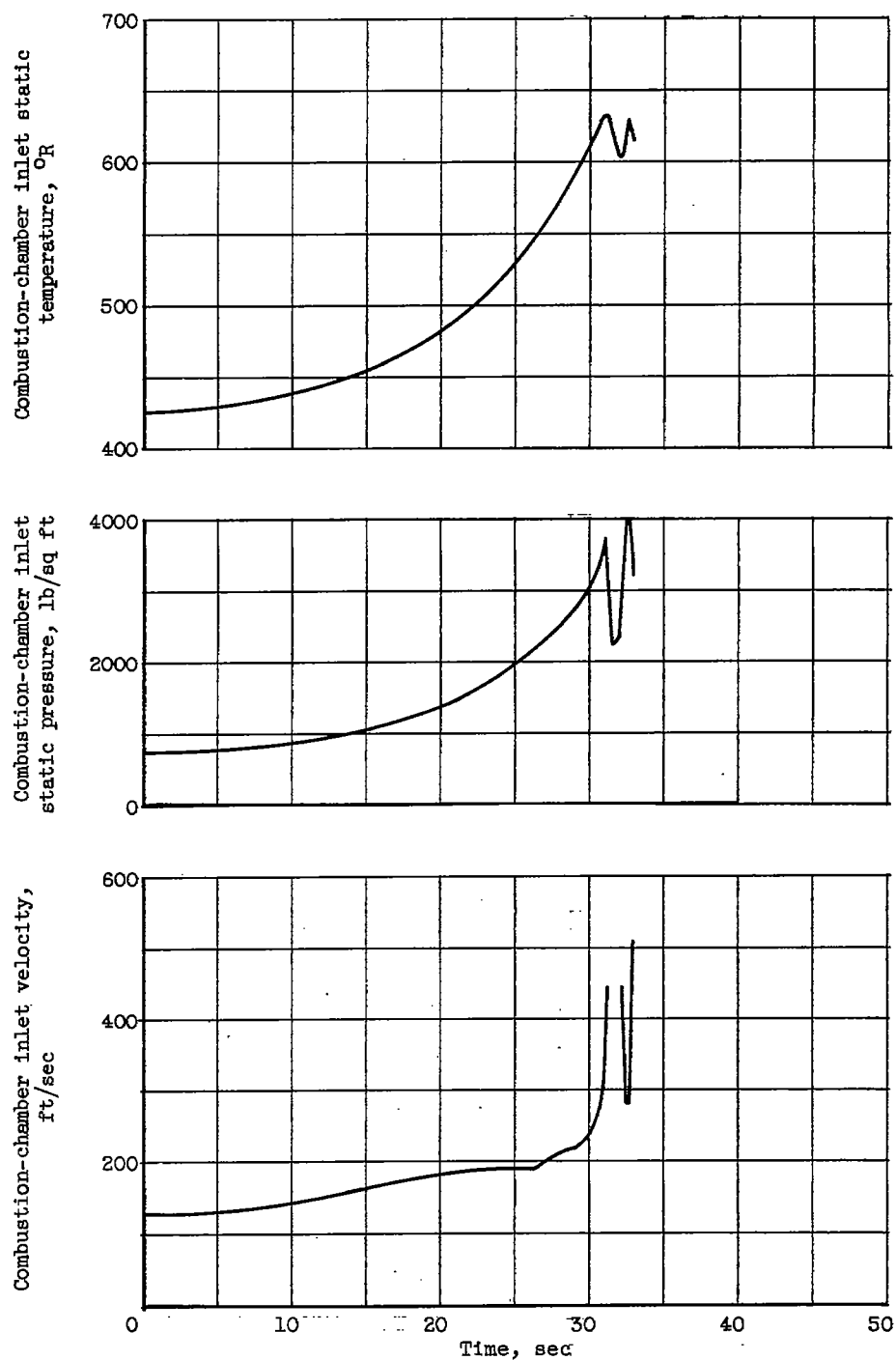
Figure 4. - Continued. Time history of flight conditions.

~~CONFIDENTIAL~~



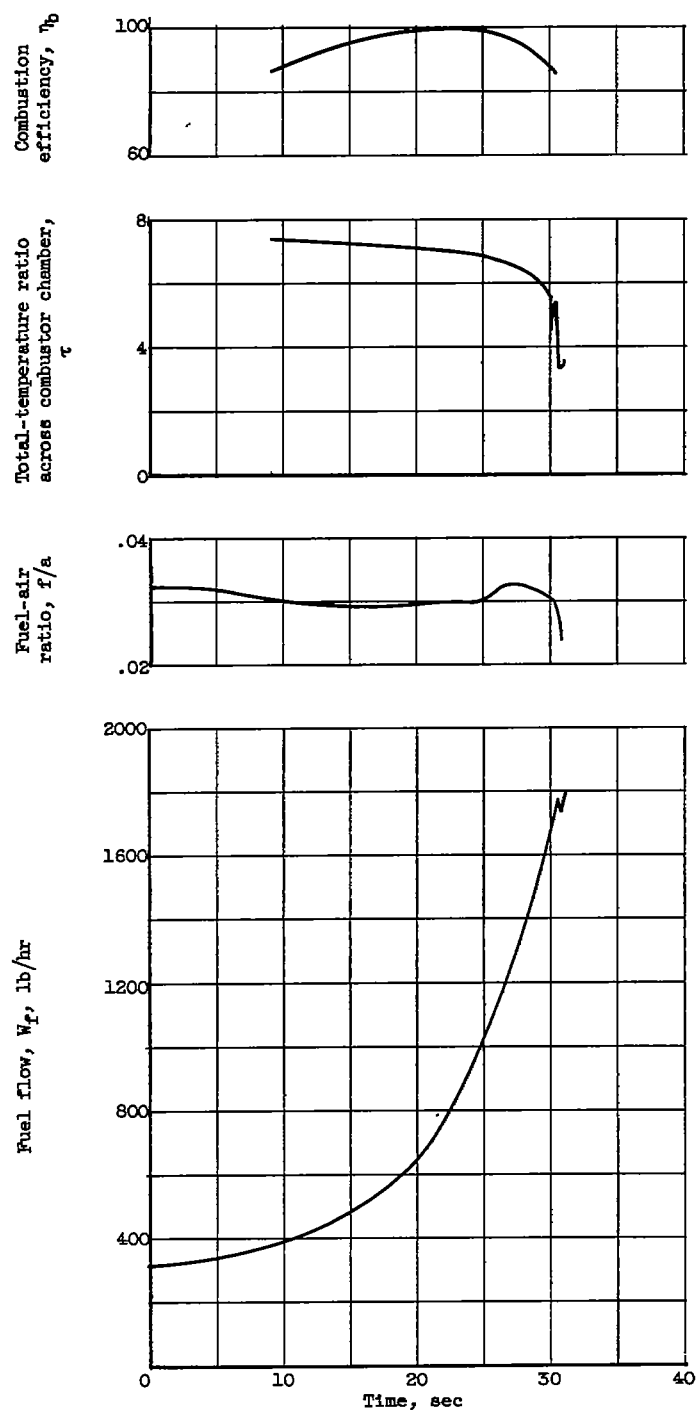
(c) Free-stream pressures and temperatures.

Figure 4. - Concluded. Time history of flight conditions.



(a) Velocity, pressure, and temperature.

Figure 5. - Time history of combustion-chamber variables.



(b) Fuel flow, fuel-air ratio, gas total-temperature ratio, and combustion efficiency.

Figure 5. - Concluded. Time history of combustion chamber variables.

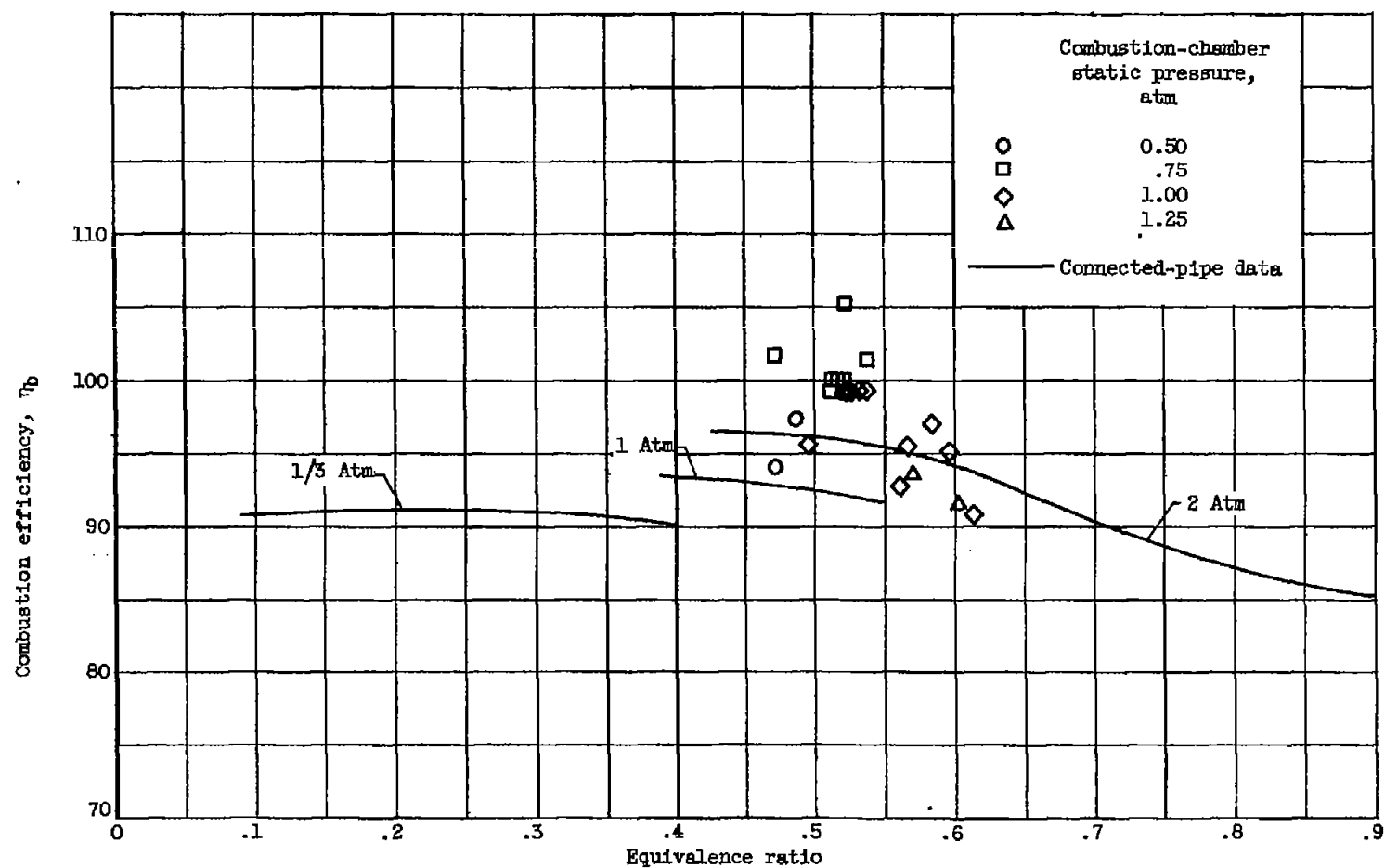


Figure 6. - Variation of combustion efficiency with equivalence ratio in connected-pipe and flight tests. Stoichiometric fuel-air ratio, 0.07635.

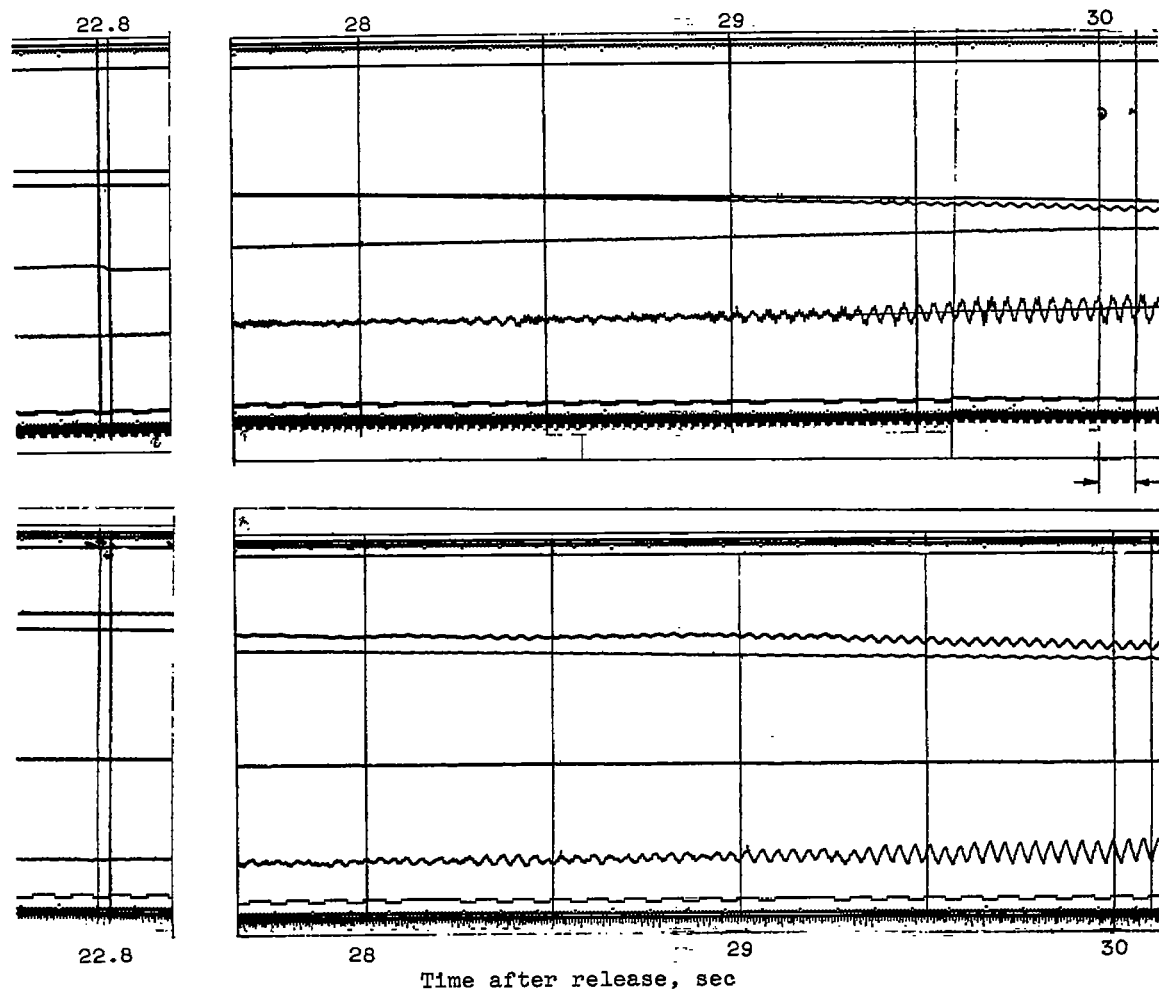
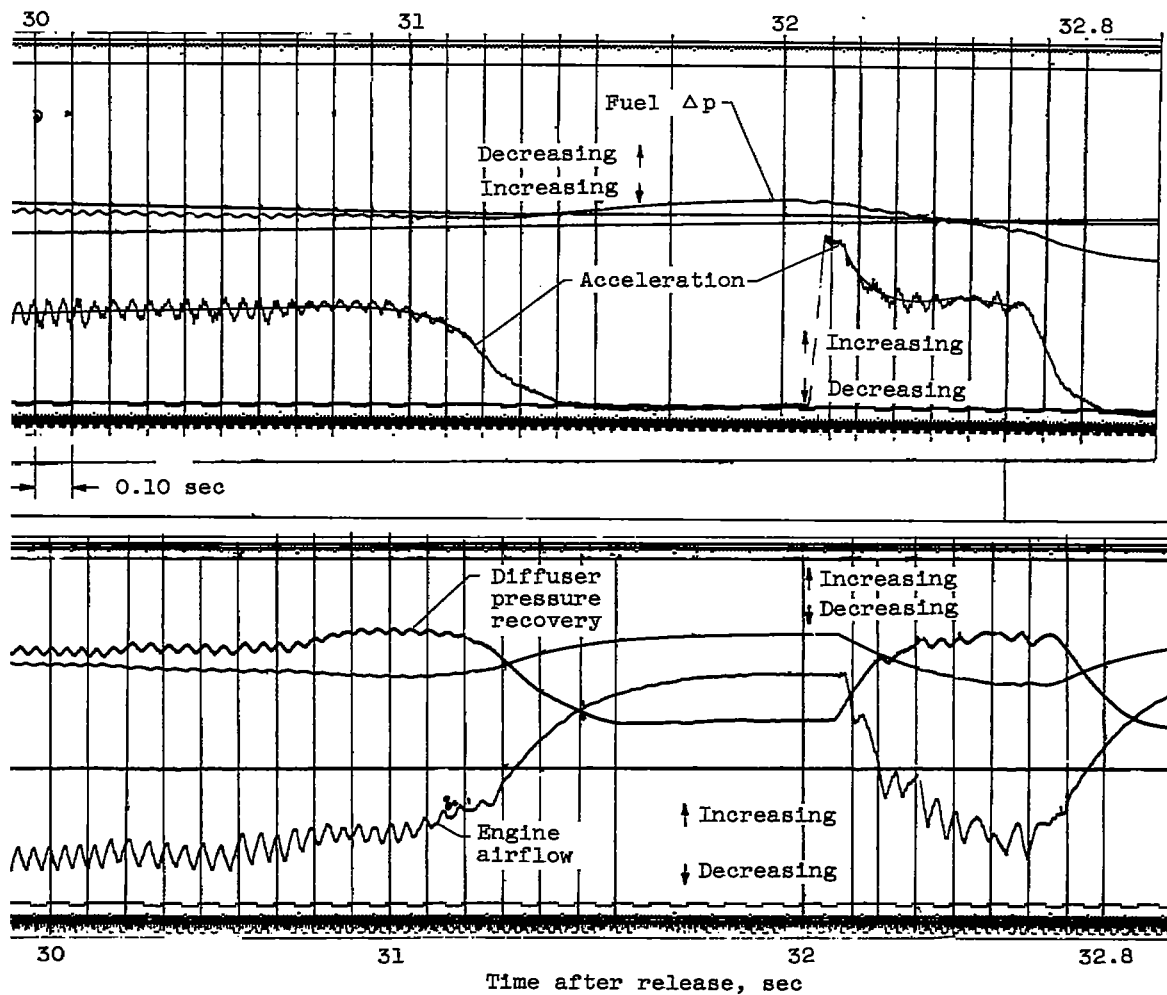


Figure 7. - Excerpts from telemeter record of



initial flight of 9.75-inch ram-jet engine.

CONFIDENTIAL

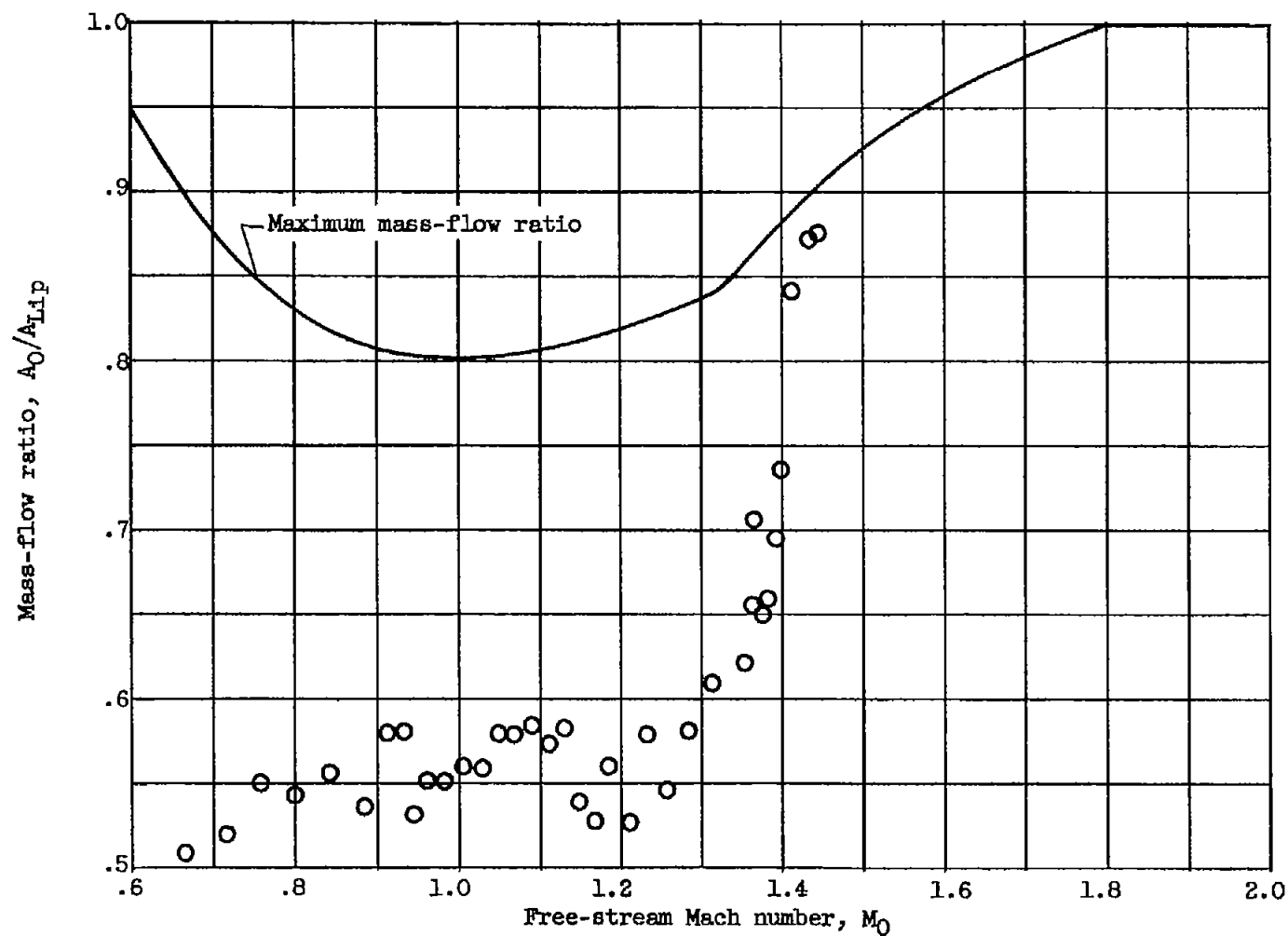


Figure 8. - Mass-Flow ratio against free-stream Mach number.

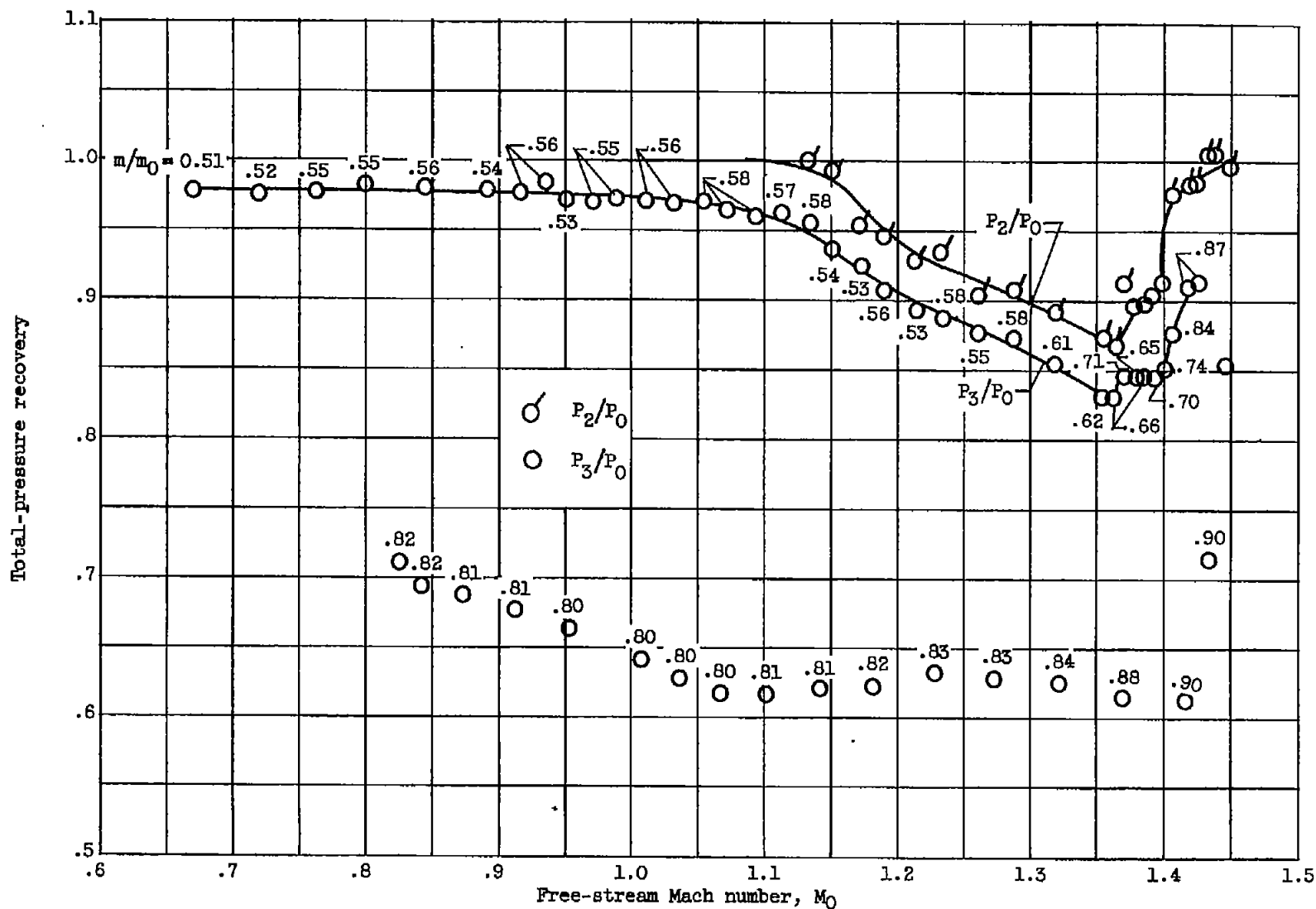


Figure 9. - Total-pressure recovery against free-stream Mach number.

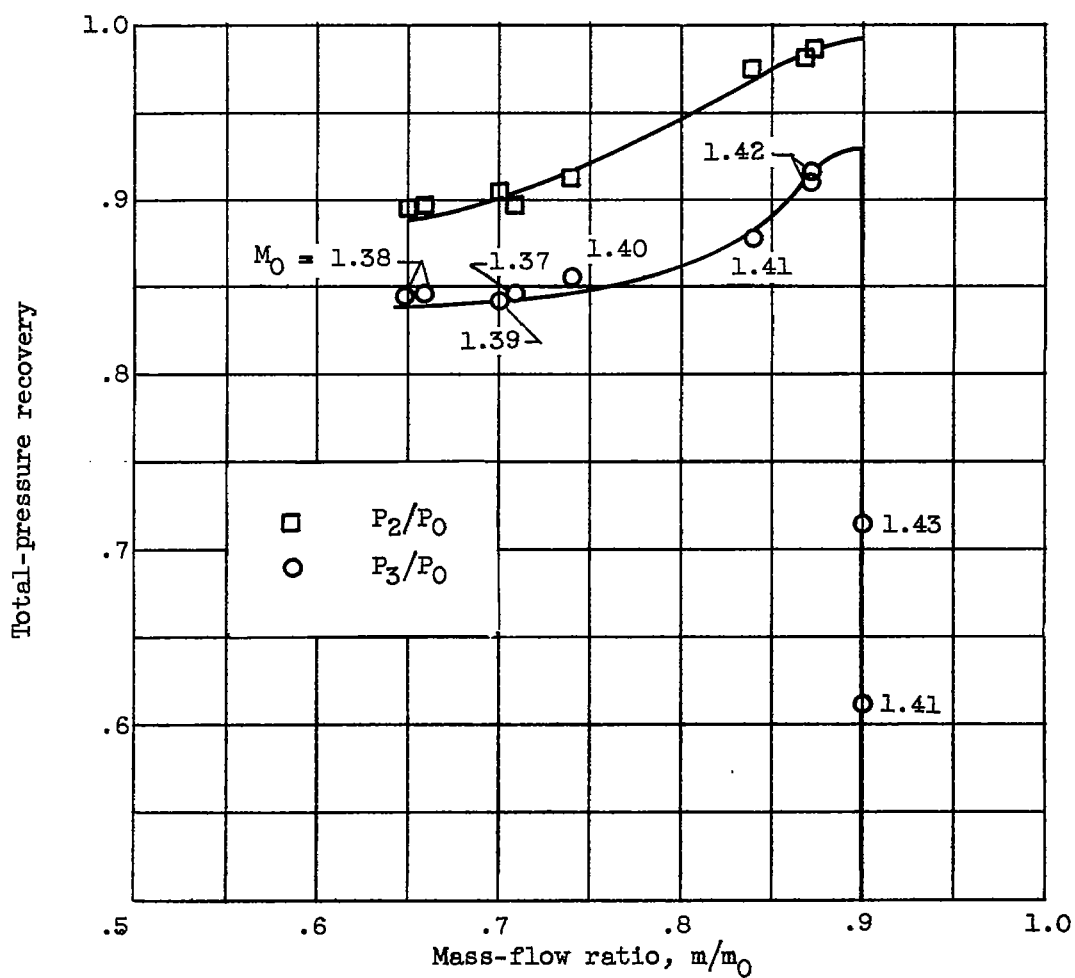


Figure 10. - Pressure recovery against mass-flow ratio at Mach number of approximately 1.40.

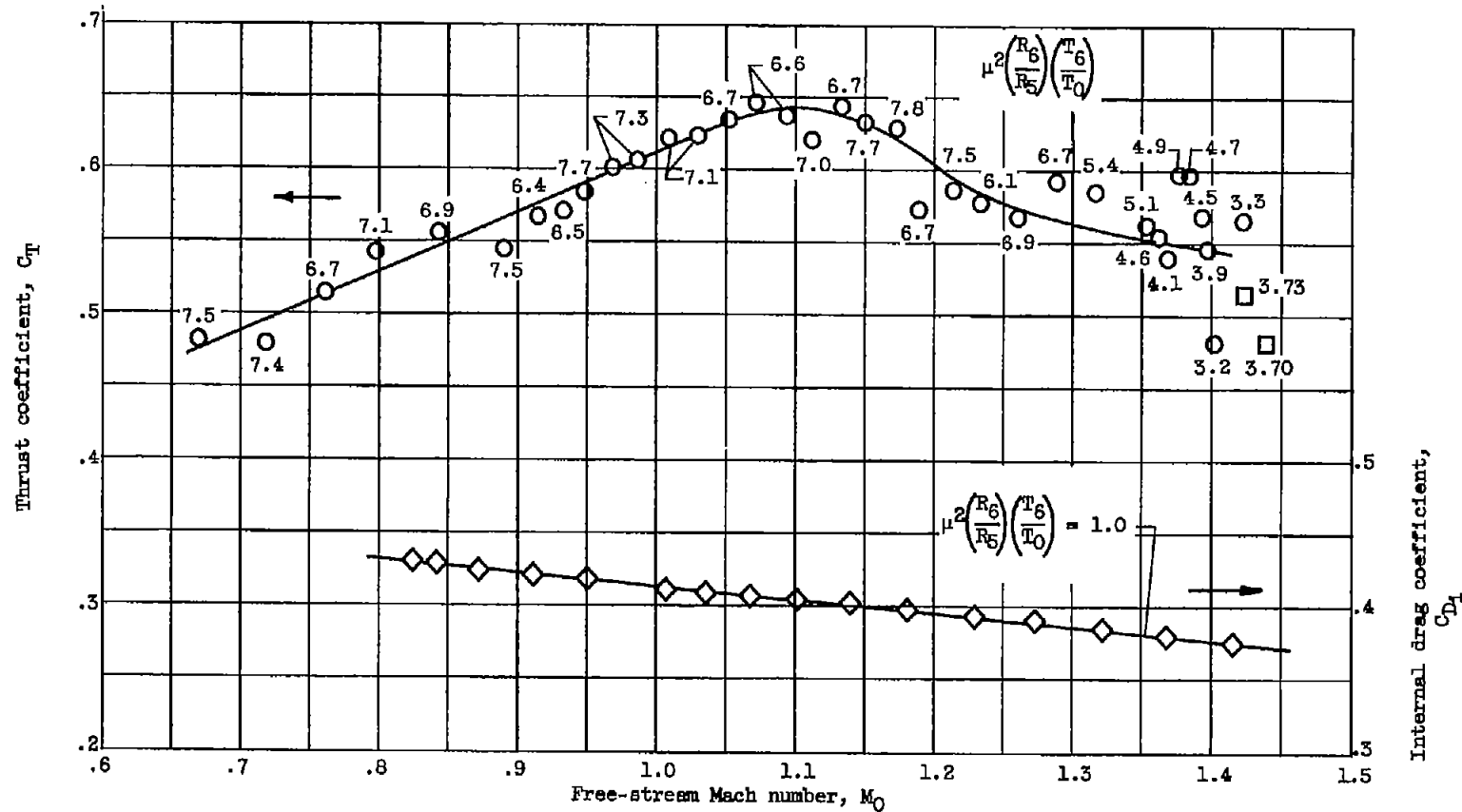


Figure 11. - Thrust coefficient and internal drag coefficient against free-stream Mach number.

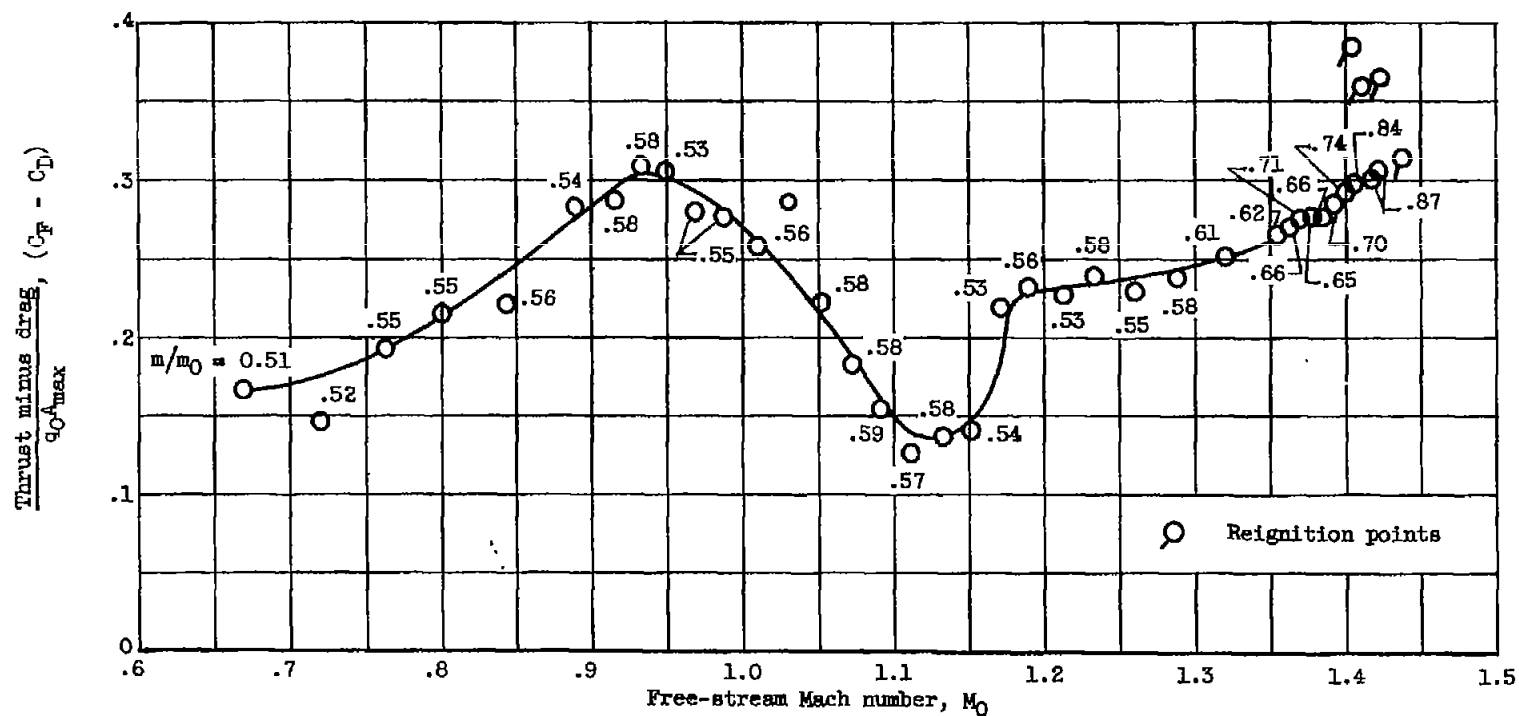


Figure 12. - Thrust-minus-drag coefficient against free-stream Mach number.

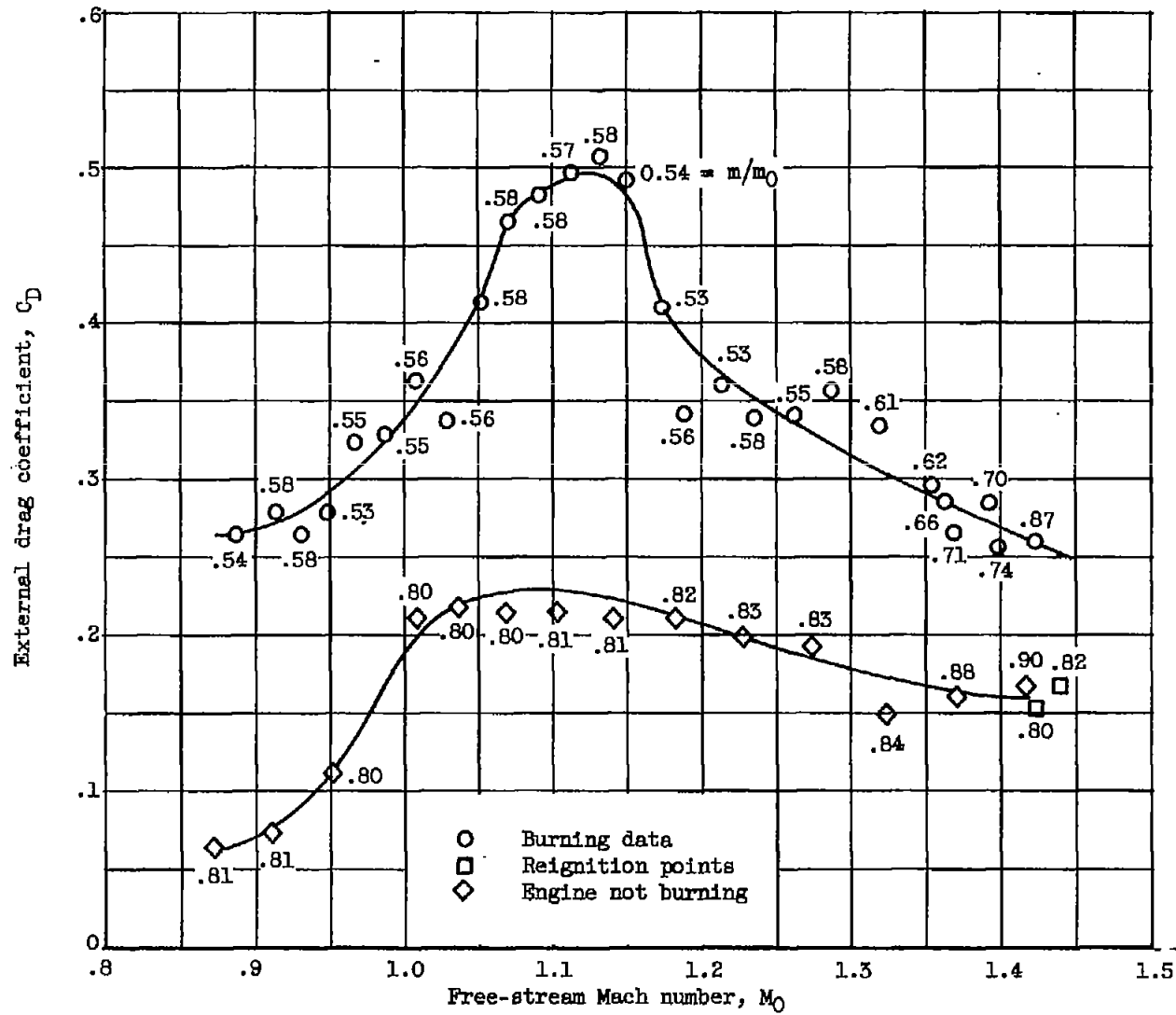


Figure 13. - External drag coefficient against free-stream Mach number.

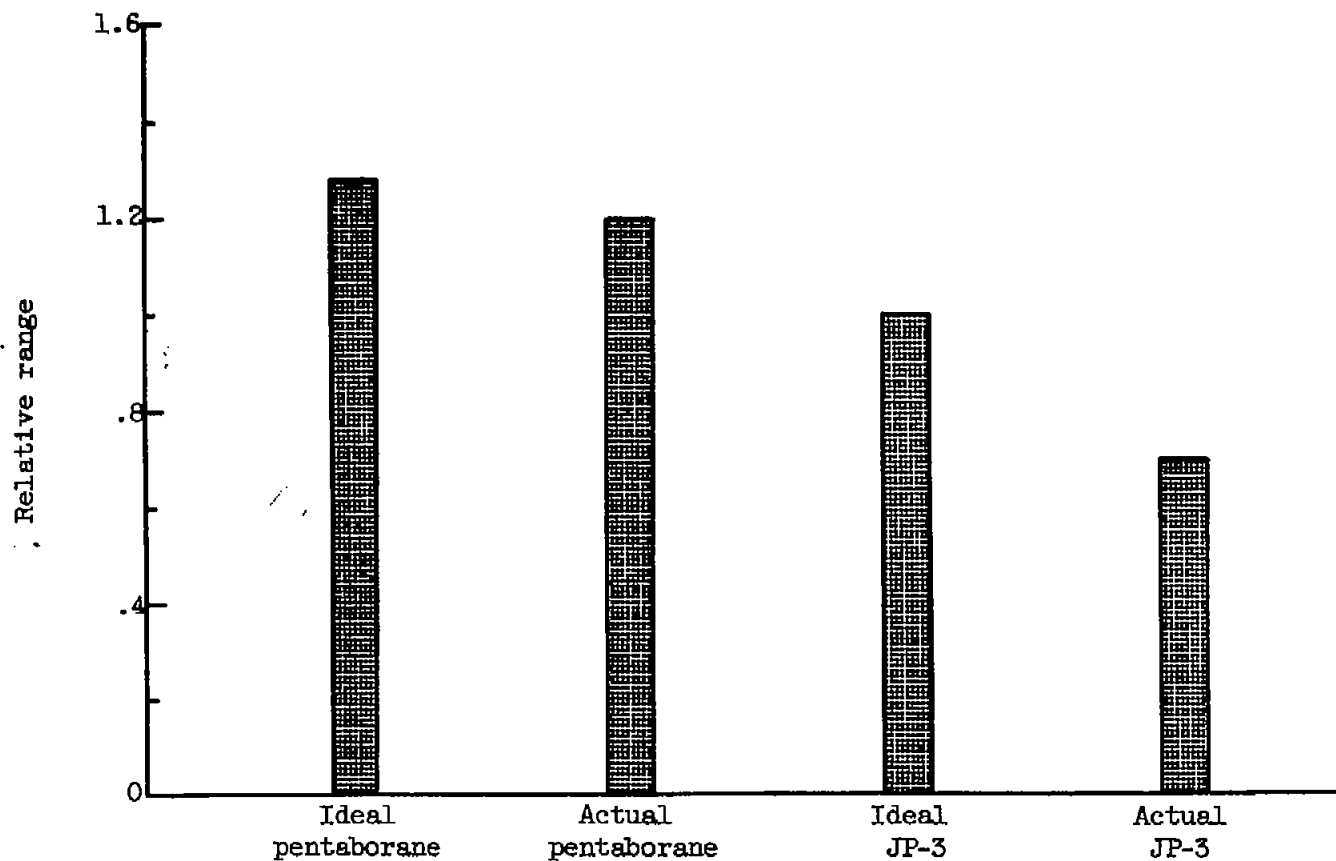


Figure 14. - Comparison of relative range for pentaborane and JP-3 fuels based on average conditions observed during flight.